Microelectronics Reliability 78 (2017) 243–248

Contents lists available at ScienceDirect

Microelectronics Reliability

journal homepage: www.elsevier.com/locate/microrel

Transition voltage of AlGaN/GaN heterostructure MSM varactor with two-dimensional electron gas

J. Osvald [a,*], G. Vanko [a], L. Chow [b], N.C. Chen [c], L.B. Chang [d,e,f]

[a] Institute of Electrical Engineering, Slovak Academy of Sciences, Dúbravská cesta 9, 841 04 Bratislava, Slovakia
[b] Department of Physics, University of Central Florida, Orlando, FL 32816-2385, USA
[c] Graduate Institute of Electro-Optical Engineering, Chang Gung University, Tao-Yuan 333, Taiwan
[d] Institute of Electro-Optical Engineering, Green Technology Research Center, Chang Gung University, Tao-Yuan 333, Taiwan
[e] Ming Chi University of Technology, New Taipei City 243, Taiwan
[f] Department of Otolaryngology Head and Neck Surgery, Chang Gung Memorial Hospital, Taoyuan 333, Taiwan

ARTICLE INFO

Article history:
Received 9 May 2017
Received in revised form 4 September 2017
Accepted 4 September 2017
Available online xxxx

Keywords:
MSM varactor
Transition voltage of MSM varactor
Voltage surge

ABSTRACT

It is not in principle clear which of the capacitors forming a varactor is responsible for the capacitance change at the transition voltage. We analyzed a theoretical case of transition voltage of the varactor formed by ideal Schottky diodes. Since real devices often do not behave strictly according to thermionic theory we also analyzed the transition voltage of experimental metal-semiconductor-metal (MSM) varactor with a two-dimensional electron gas and an MSM varactor with a dielectric layer. We found that the transition voltage of the MSM varactor was determined by the reverse-biased diode of the varactor. A voltage drop on the forward-biased diode was too low to spill over electrons in the AlGaN layer and to reduce the capacitance of the structure. The transition voltage of the MSM varactor was therefore very close to – the threshold voltage of the single diode. The situation was different with the MSM varactor with higher leakage current or in MSM varactor with the dielectric layer. The voltage drop on the forward-biased diode is no more negligible and both parts of the varactor were polarized by voltage drops on them that were caused by direct current flow. In this case, the transition voltage of the varactor was enhanced by the voltage drop on the forward-biased diode. Since the transition voltage determines the voltage region in which the varactor protect circuit devices connected in series to the varactor the presented results may help to tune this voltage region.

1. Introduction

The varactor as a voltage dependent capacitor is widely applied in oscillators, filters and frequency multipliers [1,2]. Its undisputable advantage is the ability to be directly integrated with other active semiconductor devices. The same is true for AlGaN/GaN-based varactors with a two-dimensional electron gas (2DEG), which is a very convenient structure for RF devices [3]. Varactors are, for example, used to protect another device in a circuit against voltage surge [4,5]. The degree of protection is related to the capacitance swing that is an important parameter of the varactor and is defined as the ratio between the high and the low capacitance of the varactor. A metal-semiconductor-metal (MSM) varactor consists of two Schottky diodes that are connected back to back. Application of III–V heterostructures with a 2DEG in varactors allows for devices with a wider capacitance swing. The voltage swing of the varactor, which defines the voltage range over which a device connected in series with the varactor is protected against voltage surges, is an interesting parameter [6]. However, experimental results show that technological treatment [7] changes the properties and the voltage width of the varactor only slightly.

Similarly, as in a metal-insulator-semiconductor heterojunction field-effect transistor (MISHFET), a thin dielectric layer inserted between the metal gate and the AlGaN barrier layer should reduce leakage current flowing through the device [8–10]. However, as it will be shown further, the dielectric layer also reduces the forward current [11], which has a final impact on the transition voltage of the varactor. In this paper, we analyze factors that influence the transition voltage of an MSM varactor and an MSM varactor with an insulating layer – a metal insulator semiconductor heterojunction (MISH) varactor.

Under increasing external bias, the varactor capacitance drops from a plateau value when one of the capacitances connected in series drops down. The transition voltage from the high to the low capacitance of a reverse-biased diode of the varactor depends on the Schottky barrier height, doping concentration of the AlGaN layer, AlGaN layer thickness and on Al mole fraction which is connected with the value of the polarization charge [12]. The transition voltage of the forward bias region depends principally on the same parameters. The bias voltage for the

* Corresponding author.
E-mail address: elekosva@savba.sk (J. Osvald).

http://dx.doi.org/10.1016/j.microrel.2017.09.004
0026-2714/

varactor capacitance drop was studied in [13]. Marso et al. [14] found that the transition voltage is divided between the two diodes with a ~4.1 V voltage drop on the reverse-biased diode and 0.9–1 V on the forward-biased one. It means theoretically that the reason for the capacitance transition of the varactor may be either the capacitance transition of the reverse-biased diode or that of the forward-biased diode. We study factors influencing the transition voltage of MSM and MISHFET varactors. While there are several experimental and theoretical investigations of different types of varactor, it appears that no circuit simulation of the transition voltage of varactors has yet been developed. This paper reports on a simulation study and experimental results elucidating factors that influence the transition voltage of MSM and MISHFET varactors.

2. Theory and experiment

Two Schottky diodes connected back to back which form the varactor divide external voltage to voltage drops on the forward-biased diode and the reverse-biased diode. Because of a higher resistance of the reverse-biased diode, the voltage drop is higher on this diode. It is clear that the capacitance of the diodes connected back to back may, in principle, decrease either if the voltage drop on the reverse-biased diode reaches the value at which its capacitance decreases or the voltage drop on the forward-biased diode reaches a much lower value where the forward bias diode capacitance vanishes because of the spill-over of electrons into the AlGaN layer.

For a metal semiconductor diode, the thermionic current density as a function of voltage is

$$J = J_0\left[\exp\left(\frac{qV}{nkT}\right) - 1\right], \tag{1}$$

where n is an ideality factor of the diodes and

$$J_0 = A^{**}T^2\exp\left(-\frac{q\phi}{kT}\right) \tag{2}$$

is the saturation current density and φ is the barrier height. The voltage drops on single diodes are [15]

$$V_1 = \frac{nkT}{q}\ \ln\left(\frac{J}{J_0} + 1\right), \tag{3}$$

for the forward-biased diode and

$$V_2 = -\frac{nkT}{q}\ \ln\left(-\frac{J}{J_0} + 1\right), \tag{4}$$

for the reverse-biased diode. The whole applied voltage is the

$$V = V_1 + V_2 = \frac{nkT}{q}\left[\ln\left(\frac{J}{J_0} + 1\right) - \ln\left(-\frac{J}{J_0} + 1\right)\right]. \tag{5}$$

We studied experimentally an MSM varactor prepared on an $Al_{0.25}Ga_{0.75}N$/GaN heterostructure grown on 350 μm thick silicon substrate. In contrary to previous studies, we used device topology which enabled us to measure separately electrical properties of the single diodes of the varactor. A schematic view of the experimental structure is shown in Fig. 1. A circular topology of HEMT (C-HEMT) was used. The source/drain Ohmic contacts were formed using a Nb/Ti/Al/Ni/Au metallic system, alloyed at 850 °C for 35 s. Sequential electron beam evaporation of an Ir/Al gate multilayer (7 periods of Ir/Al) followed by a top Ir layer and lift-off were carried out subsequently to form 120 nm thick ring gate contacts of variable area. The Schottky contact of our measured diode is formed by the electrode G (gate) and the Ohmic contact by the electrode D (drain) of the transistor structure. The varactor characteristics are measured between G electrodes of the diodes. The distance between the diodes forming the varactor was typically 2 mm.

We measured *I-V* and *C-V* curves at a frequency of 1 MHz of HFET capacitors between the gate and the drain of the transistor structure and the source was left floating. Varactor structures were measured between two neighbouring Schottky gates. We also studied an MSM varactor with the dielectric layer under the metal gate – analogous to a MISHFET. Therefore, we prepared metal-insulator-semiconductor

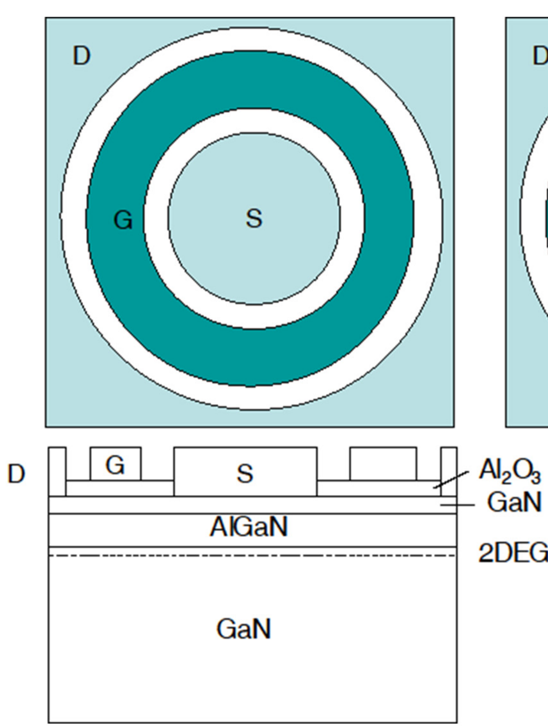

Fig. 1. View and the cross-section of the two Schottky gate capacitors forming the varactor. G is the Schottky gate and D is the Ohmic contact. Varactor is formed between the G electrodes.

(MISH) capacitors, too. The topology of the structures was the same as that of the HFET MSM varactor. The heterostructure was prepared by MO CVD technique. The thickness of the AlGaN layer with an Al mole fraction of 25% was 25 nm and that of Al_2O_3 was 20 nm, and the layer was deposited by atomic layer deposition (ALD). The gate was formed using Ni/Au metallization, and the used gate area of the MSM varactor and MSM varactors with the dielectric layer was 9.42×10^{-4} and 1.32×10^{-3} cm^2. Concentration of the 2DEG was 6×10^{12} cm^{-2} and electron mobility 2300 cm^2 V^{-1} s^{-1}. The doping concentration of AlGaN and GaN layers were estimated from a simulation to be 1×10^{15} and 1×10^{16} cm^{-3}, respectively.

3. Results and discussion

3.1. MSM varactor

The above-mentioned equations enable us to construct *I-V* characteristics of the single diodes and also the *I-V* characteristics of the whole varactor. Fig. 2 shows simulated *I-V* curves of varactors with Schottky barrier heights of 1.4 and 1.26 V. These barrier height were chosen since experimental diodes have such barriers as is shown later. In the case of the 1.4 V barrier height, two different diode ideality factors were considered. Besides the *I-V* curve of the whole structure, simulated voltage drops on the forward- and reverse-biased diodes are also shown. It is shown that for both barrier heights the voltage drop on the forward-polarized diode in the varactor is negligible compared with that of the reverse-polarized diode. For the forward-polarized diode, the voltage reaches ~0.02 V, and it does not increase further since the current is limited by the saturation current. This value was calculated for the Schottky diode with a unity ideality factor. For non-ideal thermionic transport with a higher ideality factor ($n = 3$ or $n = 3.4$), the voltage drop on the forward-biased diode may be higher but still below 0.05 V.

This calculated value of the voltage drop on the forward-biased diode is lower than the value of ~1 V assessed in Ref. [14], which is the voltage at which the capacitance of the forward-biased AlGa/GaN heterostructure vanishes. Our results show that the transition voltage of the Schottky diode varactor should be practically the same as the threshold voltage of the corresponding HEMT transistor. Merely this is true for Schottky diode contact with no or negligible leakage current of the diode. Unlike the transistor with one Schottky contact and one Ohmic contact, the Schottky diode varactor had only two identical Schottky contacts and no Ohmic contact.

We verified the results using experimental samples. Fig. 3 shows *C-V* curves of the MSM varactor together with capacitance curves of both capacitors of the varactor. For single diodes we measured a small hysteresis of the curves and for the varactor the hysteresis was approximately the sum of hysteresis of the particular diodes. Fig. 4 depicts *I-V* curves of the capacitors and the varactor. The reverse current of the diodes was very small, and it was below the sensitivity of the measurement set-up. The Schottky barrier heights of the diodes were extracted from the *I-V* curves according to [16] assuming thermionic current transport over the barrier. The barrier height of diode one was $\varphi_1 = 1.26$ V and of the diode 2 $\varphi_2 = 1.40$ V and ideality factor $n = 3$ and 3.4, respectively - the values for which the *I-V* curves were calculated. Also shown are simulated *I-V* curves of the diodes with extracted parameters from an upper part of the forward *I-V* curves.

It is seen that the transition voltage of the MSM varactor is practically the same as the threshold voltage of the capacitors. This confirms our theoretical calculation that there is a practically negligible voltage drop on the forward polarized diode. But if the reverse current is not negligible the transition voltage of the varactor is higher than the threshold voltage of the single capacitors, as was confirmed in Ref. [14].

The curves reveal an interesting feature. Although the curves of the single diodes are relatively similar, the capacitance curve of the varactor is not symmetrical with respect to the zero voltage. This effect is frequently observed in practice [1,14]. It was assumed to be caused by a non-uniformity of Schottky diodes. But this does not seem to be the reason in our case. An explanation may come from the presence of deep traps in AlGaN, GaN, and at the interface between layers of the materials [17,18]. Processes of charging and discharging the traps have very long

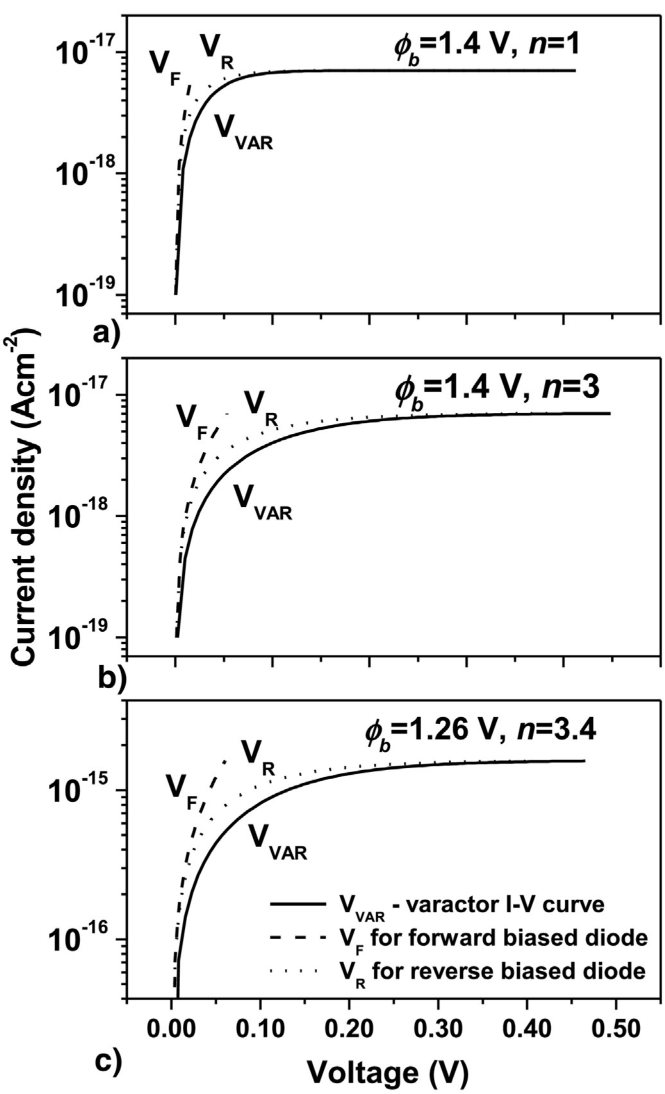

Fig. 2. *I-V* curve of a varactor with two back-to-back connected diodes and voltage drops on forward V_F and reverse V_R biased diodes for a) Schottky barrier height $\varphi = 1.4$ V and ideality factor $n = 1$ and b) $\varphi = 1.4$ V and ideality factor $n = 3$ and c) $\varphi = 1.26$ V and ideality factor $n = 3.4$.

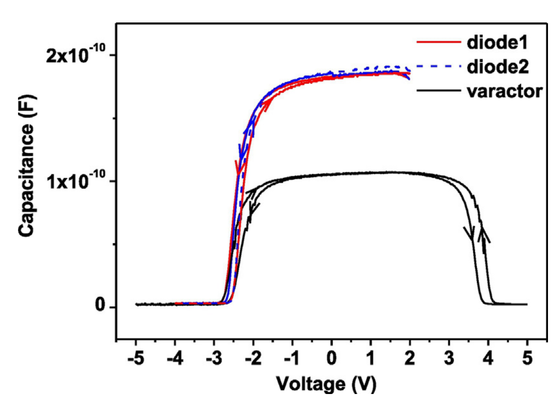

Fig. 3. *C-V* curves of single diodes of the varactor and the *C-V* curve of the varactor composed of the two diodes.

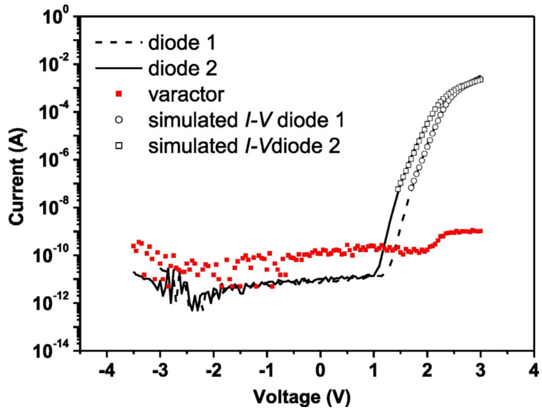

Fig. 4. *I-V* curves of the single diodes of the varactor and a *C-V* curve of the varactor composed of the two diodes.

time constants, and one may also expect a hysteresis in the capacitance curve.

The capacitance of the varactor stems from a series combination of the geometrical capacitances of the AlGaN region of both the reverse and forward biased diodes. This capacitance falls down at the bias at which one of the capacitances (with much higher probability the reverse biased diode) drops. This is connected with emptying of the 2DEG of this diode. It is also of note that the varactor capacitance is slightly higher at the plateau than that one would expect for the two equal capacitances connected in series. The capacitance of the single diodes was measured using the second Ohmic contact made on the AlGaN surface. The Ohmic contact is not present in the varactor. The Ohmic contact itself also introduced some series resistance and the potential drop on it influenced slightly the resulting capacitance [19]. In the varactor, where the Ohmic contacts are absent, the resulting combination of capacitances in series is then higher than that expected from two single capacitors in series.

3.2. MSM varactor with dielectric layer

The insertion of a dielectric layer below the gate electrode generally diminishes the leakage current of the device. Ideally, if no current flows, charges on the capacitor electrodes must be equal. The transition voltage of such a structure should be double of the threshold voltage of the single capacitor. But this is not the case in experimental structures, because of existence of the leakage current, which is always present. The external voltage is not partitioned between the diodes according to the law of electrostatics. The real transition voltage of the MISH varactor is thus lower than this value.

We measured *C-V* and *I-V* curves of two single capacitors with a 20 nm Al_2O_3 dielectric layer – MISH capacitors. It is seen in Fig. 5 that the *C-V* curves of both capacitors are very similar. Also shown is a measured *C-V* curve of the final varactor and in a part of the voltage region also a simulated *C-V* curve of the varactor from the *C-V* curves of the individual diodes. In order to obtain the simulated curve we searched for every measured (C_{i1},V_{i1}) point from the reverse part of the *C-V* curve of the first diode an equivalent measured point (C_{j2},V_{j2}) on the forward part of the second diode so, that the charge on the diodes is equal

$$C_{i1}V_{i1} = C_{j2}V_{j2}. \tag{6}$$

These two points represent at the same time one measured point of the varactor with the voltage $V_{i1} + V_{j2}$ and the capacitance $(C_{i1}C_{j2})/(C_{i1} + C_{j2})$. Here we see again higher measured capacitance than expected according to simulation the final varactor capacitance as a series connection of the two measured capacitors.

It is seen that the hysteresis of the *C-V* curves had practically no influence on the varactor transition voltage. Fig. 6 presents *I-V* curves of the two diodes separately and as back-to-back connected diodes – a varactor. The reverse current is here higher than for the Schottky diodes and it is probably a consequence of much lower barrier height (0.48 eV). The reason for this difference should be a different gate material used and technology of the gate preparation.

In this case, the *I-V* curves do not have a high rectification ratio, and there is a smaller ratio between forward and reverse currents than by an ideal Schottky diode. The ratio between the forward and reverse currents is already not so large, which means that a significant, non-negligible, voltage drop occurs also on the forward-polarized diode. This voltage drop shifts the transition voltage of the varactor (Fig. 5) to higher voltages compared with the threshold voltage of the single diodes.

The *I-V* and *C-V* curves of the single diodes and the varactor are shown again in Fig. 7 together in one plot. The *I-V* and *C-V* curves of diode 2 are shown in opposite voltage in the same way as if the diodes are connected in the varactor. Since the two diodes are not ideally equal, their *I-V* and *C-V* curves slightly differ. Additionally, the final *I-V* and *C-V* curves of the varactor are not strictly symmetrical with respect to the *y*-axis. The difference between the transition voltage of diode 1 and that of the varactor δV_1 on the left-hand side is ~1.5 V and the same difference between diode 2 and the varactor δV_2 on the right-hand side is ~1.7 V. The substantial result of this comparison is that this voltage difference is in each case equal to the voltage drop on the second forward-polarized diode. Certainly, the sum of the voltage drops equals to the voltage applied on the varactor. This experiment confirms the above-mentioned consideration that the transition voltage of the MISH varactor is higher than the threshold voltage of the appropriate MISH capacitors.

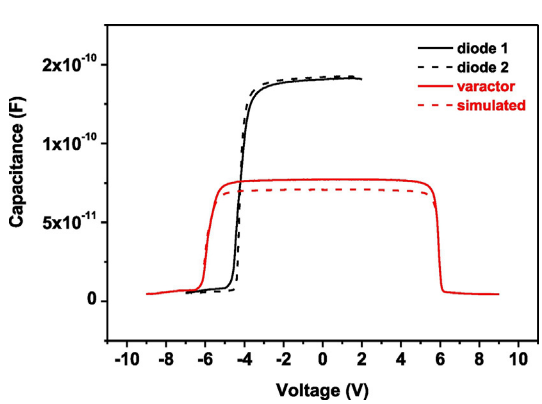

Fig. 5. *C-V* curves of single diodes with a thin dielectric layer and the varactor formed by the capacitors. Also shown is the simulated *C-V* curve of the varactor from the measured *C-V* curves of the single capacitors.

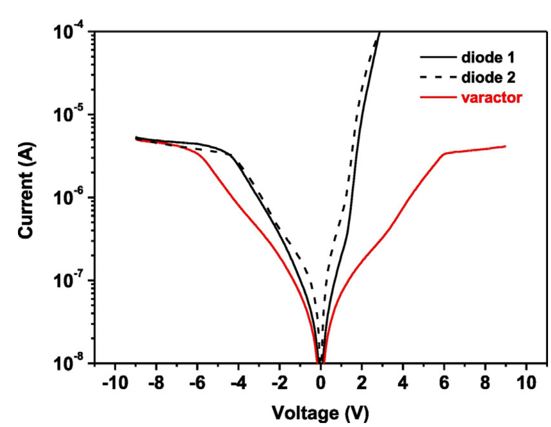

Fig. 6. *I-V* curves of the single capacitors with a thin dielectric layer and the varactor formed by the capacitors.

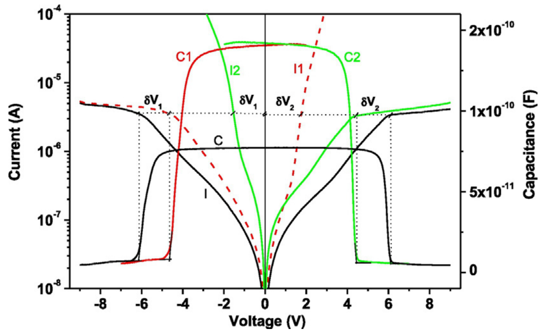

Fig. 7. *I-V* and *C-V* curves of the MSM varactor with the dielectric layer and voltage drops on the single capacitors compared with the differences between the transition voltage of the varactor and the threshold voltage of the single capacitors.

The capacitance of the MISH capacitor in forward bias commonly does not decrease to a zero value with increased forward voltage but it increases through the second capacitance step to accumulation capacitance – the geometrical capacitance of the dielectric layer [19]. To determine the actual voltage shift of the varactor transition voltage compared with that of the equivalent MISH capacitor is not simple since one has no analytical expression of the MISH capacitor current as a function of voltage unlike the one available for the current through an ideal Schottky diode varactor. But one may assume that according to the above considerations, the transition voltage of the MISHFET varactor is considerably higher than the threshold voltage of an appropriate MISHFET transistor. The measure of increase of the varactor transition voltage compared with the MISH capacitor threshold voltage increases as the rectification ratio of the diodes of the varactor is lowered. Certainly, the highest attainable transition voltage is the sum of the threshold voltages of the single diodes for the poor rectification ratio approaching unity. We would like to stress that the above considerations hold for an ideal insulator layer where no leakage current flows through the structure. But this situation could hardly be expected in real devices.

A comparison between the transition voltage of the varactor without a dielectric layer and with various dielectric films was made in Ref. [20]. The transition voltage was found to be practically the same for all structures. From the point of view of our results, it may be a consequence of a high rectification ratio of the studied structures – high ratio between the forward and reverse currents.

Both MSM and MSM varactors with the dielectric layer exhibited some degree of asymmetry in the *C-V* characteristics. Figs. 3 and 4 show that the *C-V* curves are not symmetric with respect to voltage. The effect was also observed in Ref. [1], where it was explained assuming a non-uniformity of the Schottky contacts. In our results, we even obtained different *C-V* curves and different transition voltages depending on the direction of voltage change, *i.e.* the single diodes of the varactor showed a certain degree of hysteresis. This hysteresis is connected with charges in deep traps of the semiconductor. Surprisingly we have not observed hysteresis in the transition voltage of the MISH. If there was some asymmetry in the varactor's *C-V* curve it was caused by the different properties of the diodes forming the varactor (Fig. 8). But the resulting transition voltage was practically the same for both voltage directions.

4. Conclusion

In conclusion, using the device topology which enabled us to study single diodes of the varactor, we found that the voltage of capacitance change of the varactor is determined by the threshold voltage of the reversed polarized diode of the varactor. The transition voltage of the varactor is a sum of the threshold voltage of the reverse-biased diode and the voltage drop on the forward-biased diode. In the case of an MSM varactor with a Schottky diode, there is a high rectification ratio, *i.e.* a high ratio between the forward and reverse currents. The voltage

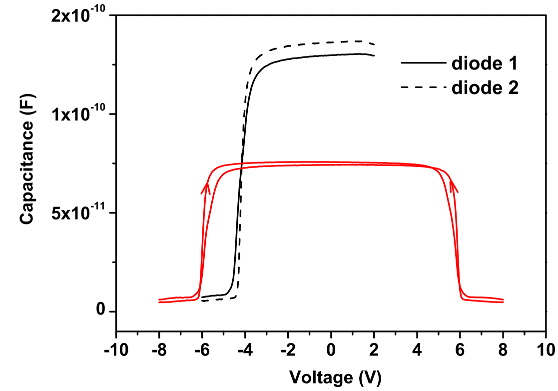

Fig. 8. *C-V* curves of the MISH varactor measured for both voltage directions. Also shown are *C-V* curves of the capacitors forming the varactor.

drop on the forward-polarized Schottky diode is negligibly small and its capacitance practically does not change. The transition voltage of the MSM varactor is then practically the same as the threshold voltage of the capacitors that form the varactor. In the case of the MSM varactor with a dielectric layer, the reverse current is expected to be lower but also the forward current is lower. The voltage drop on the forward-biased varactor is not negligible in this case. And in this case the varactor transition voltage is a sum of the threshold voltage of the reverse-polarized diode and the voltage drop on the second forward-polarized diode. This is also case for the Schottky diode with large leakage current. The ratio between forward and reverse currents determines the increase of the varactor transition voltage compared with the diode threshold voltage.

Acknowledgements

The author are thankful for the financial support received during work on this study from the Slovak Grant Agency for Science under Contract No. 2/0112/17, Agency for Research and Development APVV-14-0613.

References

[1] S.H. Shin, D.M. Geum, J.H. Jang, MSM varactor diodes based on $In_{0.7}Ga_{0.3}As$ HEMTs with cut-off frequency of 908 GHz, IEEE Electron Device Lett. 35 (2014) 172–174.
[2] D.M. Geum, S.H. Shin, S.M. Hong, J.H. Jang, Metal semiconductor-metal varactors based on InAlN/GaN heterostructure with cutoff frequency of 308 GHz, IEEE Electron Device Lett. 36 (2015) 306–308.
[3] L.B. Chang, A. Das, R.M. Lin, S. Maikap, M.J. Jeng, S.T. Chou, An observation of charge trapping phenomena in GaN/AlGaN/Gd_2O_3/Ni-Au structure, Appl. Phys. Lett. 98 (2011) 222106.
[4] Ch.Y. Tien, P.-Y. Kuei, L.,B. Chang, Improved surge protection of flip-chip gallium nitride-based HEMTs by metal-semiconductor-metal two-dimensional electron gas varactor, J. Vac. Sci. Technol. B 33 (2015) 021401.
[5] Y.Ch. Ferng, L.B. Chang, A. Das, Ch.Ch. Lin, Ch.Y. Cheng, P.Y. Kuei, L. Chow, Improvement of surge protection by using an AlGaN/GaN-based metal-semiconductor-metal two-dimensional electron gas varactor, Jap. J. Appl. Phys. 51 (2012) 124201.
[6] Ch.M. Anderson, N. Ejebjörk, A. Henry, S. Andersson, E. Janzé, H. Zirath, N. Rorsman, et al., IEEE Electron Device Lett. 32 (2011) 788–790.
[7] Y.Ch. Ferng, L.B. Chang, A. Das, C.Y. Cheng, C.C. Lin, Effective treatment on AlGaN/GaN MSM-2DEG varactor with $(NH_4)_2S/P_2S_5$ solution, Electrochem. Solid-State Lett. 10 (2010) H350–H353.
[8] V. Adivarahan, M. Gaevski, W.H. Sun, H. Fatima, A. Koudymov, S. Saygi, G. Simin, J. Yang, M.A. Khan, A. Tarakji, M.S. Shur, R. Gaska, Submicron gate Si_3N_4/AlGaN/GaN-metal-insulator-semiconductor heterostructure field-effect transistors, IEEE Electron Device Lett. 24 (2003) 541–543.
[9] S. Arulkumaran, T. Egawa, H. Ishikawa, Jap. J. Appl. Phys. 44 (2005) L812.
[10] K. Balachander, S. Arulkumaran, T. Egawa, Y. Sano, K. Baskar, Demonstration of AlGaN/GaN metal-oxide-semiconductor high-electron-mobility transistors with silicon oxy-nitride as the gate insulator, Mater. Sci. Eng., B 119 (2005) 36–40.
[11] Liu Ch, E.F. Chor, L.S. Tan, Investigations of HfO_2/AlGaN/GaNHfO_2/AlGaN/GaN metal-oxide-semiconductor high electron mobility transistors, Appl. Phys. Lett. 88 (2006) 173504.
[12] J. Osvald, Influence of AlGaN/GaN heterojunction parameters on its capacitance voltage characteristics, J. Appl. Phys. 106 (2009), 013708. .

[13] M. Marso, M. Wolter, P. Javorka, A. Fox, P. Kordoš, AlGaN/GaN varactor diode for integration in HEMT circuits, Electron. Lett. 37 (2001) 1476–1478.
[14] M. Marso, A. Fox, G. Heidelberger, P. Kordoš, H. Lüth, Comparison of AlGaN/GaN MSM varactor diodes based on HFET and MOSHFET layer structures, IEEE Electron Device Lett. 27 (2006) 945–947.
[15] J. Osvald, Back-to-back connected asymmetric Schottky diodes with series resistance as a single diode, Phys. Status Solidi A 212 (2015) 2754–2758.
[16] J. Osvald, E. Dobročka, Generalized approach to the parameter extraction from I–V characteristics of Schottky diodes, Semicond. Sci. Technol. 11 (1996) 1198–1202.
[17] P. Dianat, R.W. Prusak, E. Gallo, A. Cola, A. Persano, F. Quarant, B. Nabel, A highly tunable heterostructure metal-semiconductor-metal capacitor utilizing embedded 2-dimensional charge, Appl. Phys. Lett. 100 (2012) 153505.
[18] J. Osvald, Simulation of the influence of interface states on capacitance characteristics of insulator/AlGaN/GaN heterojunctions, Phys. Status Solidi A 210 (2013) 1340–1344.
[19] P. Chattopadhyay, B. Ray Chaudhuri, Frequency dependence of forward capacitance-voltage characteristics of Schottky barrier diodes, Solid State Electron. 36 (1993) 605–610.
[20] Ch.Y. Tien, P.Y. Kuei, L.B. Chang, Ch.P. Hsu, Capacitance swing and capacitance ratio of GaN-based metal-semiconductor-metal two-dimensional electron gas varactor with different dielectric films, J. Electr. Eng. Technol. 10 (2015) 1720–1724.